Modeling the 10,000-Year Geomagnetic Disturbance Scenarios Based on Extreme Value Analysis

IEEE EMC SOCIETY | Letters on Electromagnetic Practice and Applications

Modeling the 10,000-year Geomagnetic Disturbance Scenarios Based on Extreme Value Analysis

Min-zhou Liu, *Student Member, IEEE*, Yan-zhao Xie, *Senior Member, IEEE*, Yu-hao Chen and Qing Liu

***Abstract*—Modeling the extreme geomagnetic disturbance (GMD) scenarios is of great significance for risk assessment of the power system. In this paper, we model the 10,000-year GMD scenarios using the extreme value analysis to complement the classical 100-year and 200-year events. The 10,000-year GMD event is required for safety-critical nodes such as the ultra-high voltage (UHV)/extra-high voltage (EHV) substations and nuclear power plants, etc. The return level of geomagnetic variation is estimated using the geomagnetic observations based on extreme value theory, which is then combined with the theoretical upper limit of the disturbance storm time (Dst) index to establish the 10,000-year GMD scenarios. Finally, we present an application example of 10,000-year geomagnetically induced currents (GICs) in the Sanhua UHV power grid.**

***Index Terms*—extreme value theory, geoelectric field, geomagnetic disturbances, geomagnetically induced currents, largest imaginable magnetic storm, ultra-high voltage power grid.**

I. INTRODUCTION

Geomagnetic disturbances (GMDs) initiated by solar activities induce geoelectric fields on the Earth's surface and consequently drive geomagnetically induced currents (GICs) in the high-voltage power grid. GICs give rise to half-cycle saturation of the transformers, causing hot spot heating, increased reactive power loss and harmonics injection, which may pose a threat to the reliability of the electrical equipment and the power grid [1]-[3]. In this respect, it is of great significance to construct typical GMD scenarios to provide guidance for risk assessment of power system in engineering practice.

Digital geomagnetic data with sampling period of 1-minute or even smaller have been collected for decades worldwide; however, it is usually necessary to consider more serious GMD scenarios for risk assessment. The extreme value analysis (EVA) is widely adopted for generating the 100-year and 200-year GMD events for North America [4] and Europe [5], etc. However, these classical events are not sufficient for critical nodes such as the UHV/EHV substations and nuclear power plants. In recent years, the 10,000-year GMD event has been concerned by researchers and adopted by engineering standards [6]-[7].

This work is supported by National Key R&D Program of China under Grant 2016YFC0800100. *(Corresponding author: Yan-zhao Xie.)*

The authors are with the State Key Laboratory of Electrical Insulation and Power Equipment, National Center for International Research on Transient Electromagnetics and Applications, School of Electrical Engineering, Xi'an Jiaotong University, Xi'an 710049, China (e-mail: liuminzhou@outlook.com; yzxie@mail.xjtu.edu.cn; chenyuhao@stu.xjtu.edu.cn).

Q. Liu is also with the College of Electrical and Control Engineering, Xi'an University of Science and Technology, Xi'an 710054, China (e-mail: liuqing623nn@163.com).

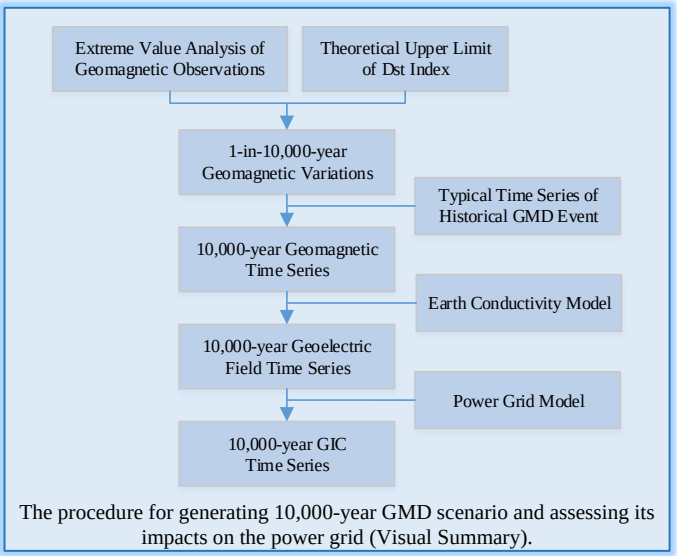

The procedure for generating 10,000-year GMD scenario and assessing its impacts on the power grid (Visual Summary).

In this study, we model the 10,000-year GMD event using the extreme value analysis and then assess the GIC in the power grid. Although located at low latitudes, the 1000 kV Sanhua UHV power grid with long transmission lines and small DC resistances may be subjected to large GIC levels [8]-[9]. For illustration, a case study of the 1000 kV Sanhua UHV power grid under 10,000-year GMD scenario is carried out.

II. METHODS OF GENERATING THE 10,000-YEAR GMD SCENARIOS

A. The Procedure for Generating the 10,000-year GMD Scenario and Assessing its Impacts on the Power Grid

Here is a brief introduction to the procedure for generating the 10,000-year GMD scenario and assessing its impacts on the grid, as shown in the visual summary. Firstly, the 10,000-year geomagnetic variation is estimated by combining the EVA and theoretical upper limit of GMD. Then, the largest historical GMD event observed is scaled according to the peak geomagnetic variation. Finally, the 10,000-year geoelectric field and GIC levels are evaluated based on the earth conductivity model and power grid model.

Take-Home Messages:

- The 10,000-year GMD scenario is required for risk assessment of critical assets in power grids such as the UHV/EHV substations and nuclear power plants.
- The 10,000-year return level of geomagnetic variation is estimated using the extreme value analysis of geomagnetic observation and theoretical upper limit of Dst index.
- UHV power grids may be subjected to large 10,000-year GICs, which requires appropriate mitigation measures.

B. Extreme Values Analysis of Geomagnetic Observation

Extreme statistical analysis, especially the generalized Pareto distribution (GPD), is widely used to estimate the occurrence of extreme GMD scenarios, whose cumulative probability distribution function is as shown in equation (1).

$$G(x;\mu,\sigma,\xi)=1-\left(1+\xi\frac{x-\mu}{\sigma}\right)^{-1/\xi}, \quad (x\geq\mu, 1+\xi\frac{x-\mu}{\sigma}>0) \tag{1}$$

where, x is the random variable; μ denotes the location parameter (i.e., threshold), ξ and σ represents the shape parameter and the scale parameter, respectively.

During the GPD modeling process, observed data exceeding a certain threshold are selected, resulting in only a small amount of data available for parameter estimation. The estimates and confidence intervals for GPD model parameters can be obtained using the maximum likelihood estimation method [10]-[11].

In fact, there exists uncertainty in the estimation of the return level by EVA due to the small sample size. The Wald confidence interval is used to characterize the uncertainty of the return level, which is based on the asymptotic normality of the parameter estimators.

C. Theoretical Upper Limit for Dst Index

Reference [12] proposed the theoretical upper limit for the largest imaginable geomagnetic storm, corresponding to the value of Dst index of -2500 nT, which has been adopted by some studies on GICs in the UK power grids [6], [13].

The Dst index indicates the strength of the ring current, which is one of the main sources of GMD at low latitudes. Thus, the upper limit of the Dst index provides a valuable reference for GIC study in China.

D. Modeling the Geoelectric Field and GIC

The plane wave method [1] has been proved to be suitable for low latitude areas. The geoelectric field $\boldsymbol{E}$ on the earth surface can be obtained by combining the geomagnetic field $\boldsymbol{B}$ with the surface impedance $\boldsymbol{Z}_0$ in the frequency domain according to equation (2). For 1D layered earth model, the surface impedance can be solved recursively using the thickness and conductivity parameters of each layer.

$$\begin{bmatrix}E_x(\omega)\\E_y(\omega)\end{bmatrix}=\frac{1}{\mu_0}\begin{bmatrix}0 & Z_0(\omega)\\-Z_0(\omega) & 0\end{bmatrix}\begin{bmatrix}B_x(\omega)\\B_y(\omega)\end{bmatrix} \tag{2}$$

where, sub-x and sub-y refer to the components in the north and east directions.

The geoelectric field induced by the GMD can be modeled as an equivalent voltage source on the transmission lines. GIC can usually be regarded as quasi-direct currents, and only the DC resistance parameters of components in a power grid are considered, so the GIC in a power grid can be solved by the circuit analysis. In this study, the Lehtinen-Pirjola (LP) method [14] is used to calculate the GIC flowing into the earth in each substation according to equation (3).

$$\boldsymbol{I}=(\boldsymbol{1}+\boldsymbol{YZ})^{-1}\cdot\boldsymbol{J} \tag{3}$$

where, $\boldsymbol{Y}$ denotes the network admittance matrix, $\boldsymbol{Z}$ is the earthing impedance matrix, and $\boldsymbol{J}$ is the current source vector.

III. 10,000-YEAR GMD SCENARIOS FOR SANHUA AREA

A. Geomagnetic Observation in Sanhua Area

The 1-minute geomagnetic data at Beijing Ming Tombs (BMT, 40.3 ℕ 116.2 ℇ) observatory from 1996 to 2019 are used for EVA. Compared with other observatories in China, BMT has the advantages of closer distance to the Sanhua UHV grid, relatively higher latitude and longer measurement time. Moreover, the BMT data are representative since the spatial distribution of geomagnetic variation at low latitude is relatively uniform [15]. However, for high latitude areas, it is necessary to use averaging or interpolation methods to integrate the geomagnetic data from multiple observatories at the similar geomagnetic latitude, since the spatial distribution of geomagnetic variation is much more complicated.

The geomagnetic data from SuperMAG have already removed the annual and daily baselines to reduce the impacts of other interferences [16]. The historical time series of variation ΔB are shown in Fig. 1. Some statistical results about BMT data are provided in Table 1. As some studies on sudden impulse storms have pointed out, the 1-minute data used in this study may not be able to fully capture high-frequency variations [17]-[19], which will be considered in future studies.

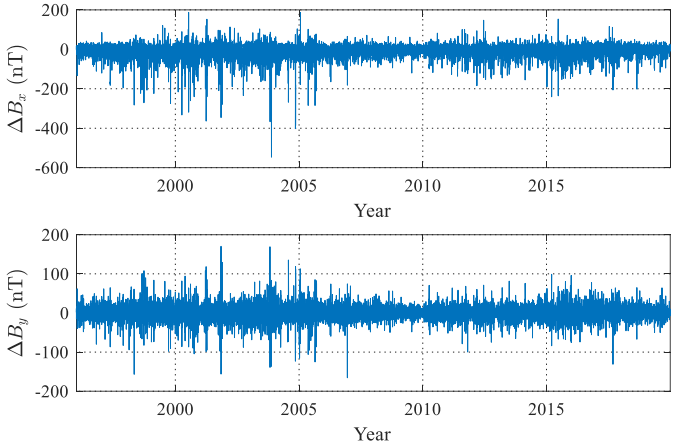

Fig. 1. Time series of the geomagnetic variations in the north and east directions at BMT observatory from 1996 to 2019.

Table 1: Maximum Variation and Rate-of-change of Geomagnetic Field Observed at BMT

Component	max(|ΔB_i|) (nT) (i=x, y, H)	max(|dB_i/dt|) (nT/min)
Northward B_x	546	130
Eastward B_y	170	85
Horizontal B_H	547	132

B. Estimating Geomagnetic Variation Using Extreme Value Analysis

Both the magnitude of variation and rate-of-change of the magnetic field can characterize the intensity of GMD, and the former is adopted for EVA in this study. Before performing parameter estimation for the Pareto distribution, some data preprocessing is needed, including threshold selection and data declustering [4].

The selection of the threshold is relatively subjective but a key issue. That is, if the threshold is too large, there are only a few excesses, then the variance of the estimator is larger; if the threshold is too small, the distribution of the excesses may be different from the GPD, resulting in a biased estimate. Therefore, it is necessary to take into account the

relationship between the bias and the variance for threshold selection. In this study, the 0.9997 quantile of the geomagnetic variation is used as the threshold.

Moreover, we decluster the geomagnetic data above the threshold to eliminate the dependency between data, which means extremes separated by fewer than 12 h non-extremes belong to the same cluster, and only the maximum in each cluster is considered.

The 'extRemes' package in R is used in this study [8]. The 100, 200 and 10,000-year return levels for the geomagnetic variation and corresponding confidence intervals at BMT observatory are shown in Table 2 and Fig. 2. In this study, the magnetic variation and GIC estimates are rounded to the nearest ten digits. From Fig. 2, we can observe that there is a large uncertainty in the estimation of the 10,000-year return level. This can be explained by the fact that the digital geomagnetic data are only available for a few decades. The upper bound of 95% Wald confidence interval is adopted to account for modeling uncertainties.

Table 2: Return Level and Confidence Interval of Magnetic Variation at BMT

Return Period (year)	Return Level (nT)	95% Confidence Interval (nT)
100	570	[330, 810]
200	620	[290, 950]
10,000	910	[-120, 1930]

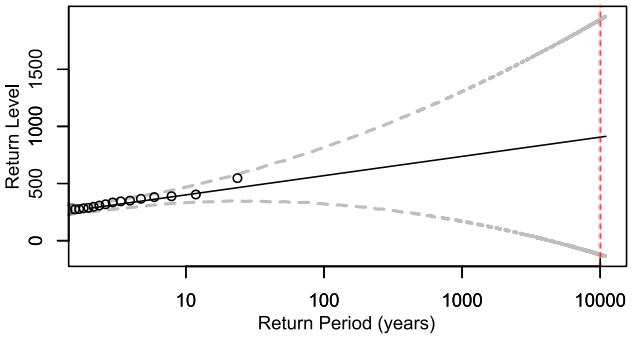

Fig. 2. The return level (black curve) of horizontal magnetic variation at BMT and its 95% Wald confidence interval (gray dashed curves). (The circles indicate the empirical return level, and the red dashed line represents the 10,000-year return period.)

C. Theoretical Upper Limit of Magnetic Variation in Sanhua Area

The geomagnetic variation estimates based on the Dst index can provide scale factors to study the 1-in-10,000-year extreme event. Assuming a simple dipolar ring current model on the plane of geomagnetic equator [13], the horizontal geomagnetic variation at geomagnetic latitude φ can be simplified as $\Delta B_H \cos(\varphi)$, where ΔB_H is the horizontal geomagnetic variation on the geomagnetic equator. The upper limit of geomagnetic variation at BMT observatory is 2150 nT, which is larger than the upper bound of 95% Wald confidence interval of 10000-year scenarios.

For Sanhua area, the geomagnetic latitude ranges from 15.06~33.88 ℕ, and the corresponding upper limit of geomagnetic variation is 2080~2410 nT.

Taking into account all the above-mentioned elements, 1930 nT estimated by EVA is used in the following GIC study since it has not reached the theoretical upper limit. The theoretical upper limit 2410 nT may be adopted if more conservative situations need to be considered.

D. 1-in-10,000-year Geomagnetic Time Series

A typical historical GMD event at BMT observatory that occurred on July 15-16, 2000 shown in Fig. 3, is chosen for the following GIC study, which is scaled to 1930 nT for 10,000-year scenario, resulting in a scale factor of 6.0.

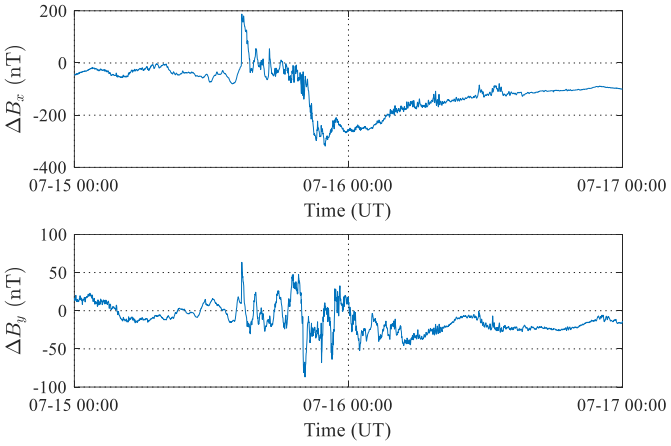

Fig. 3. Time series of the geomagnetic variations at BMT observatory during the GMD event occurred on July 15-16, 2000.

IV. Results of 10,000-year Geoelectric Field and GIC in Sanhua UHV Grid

A. Results of Geoelectric Field in Sanhua Area

The 1-D layered earth conductivity model, as shown in Table 3 [9], is used for modeling the geoelectric field in Sanhua area based on the plane wave method. The results of geoelectric field are shown in Fig. 4, with a peak value of 0.37 V/km.

Table 3: 1-D Layered Earth Conductivity Model for Sanhua Area

Layer	Resistivity ρ (Ω m)	Thickness d (km)
1	2000	30
2	770	60
3	2000	60
4	3	∞

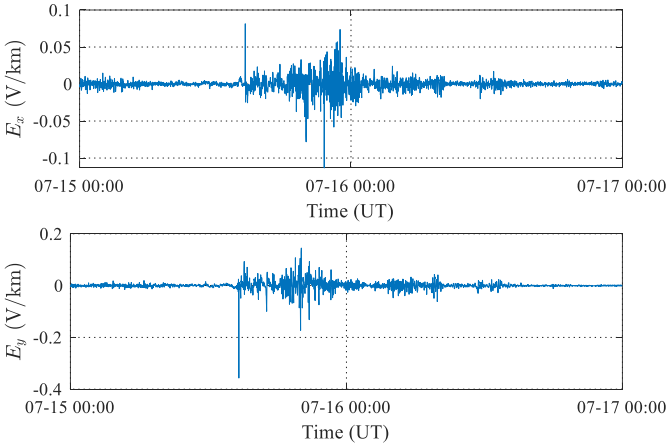

Fig. 4. Time series of northward and eastward geoelectric fields for Sanhua area during July 15-16, 2000.

B. Characteristics of 10,000-year GICs in Sanhua Grid

The planned Sanhua UHV power grid is used as the test case, which includes 36 substations and 46 lines [9]. Assume that there are two

transformers in each substation, and the DC resistances of the series winding and common winding are 0.1827 and 0.1415 Ω, respectively. Moreover, the grounding resistance is 0.1 Ω for all substations.

The spatial distribution and time-varying characteristics of the GIC in the typical historical magnetic storm scenario are evaluated, as shown in Fig. 5 and Fig. 6. The nodes with large GIC are located at the edges and "corners" of the UHV grid, and the largest three-phase GIC is 137 A at Shanghai substation, which verifies the "corner effect" [20]. By scaling the above results, the largest and the average 10,000-year GICs in Sanhua UHV grid are 830 A and 300 A, respectively. For critical nodes in the UHV grid, appropriate mitigation measures need to be taken, since the possible GICs exceed the common threshold of the transformer in engineering standards, such as 75 A/phase of effective GIC in North American Electric Reliability Corporation (NERC) standard [21].

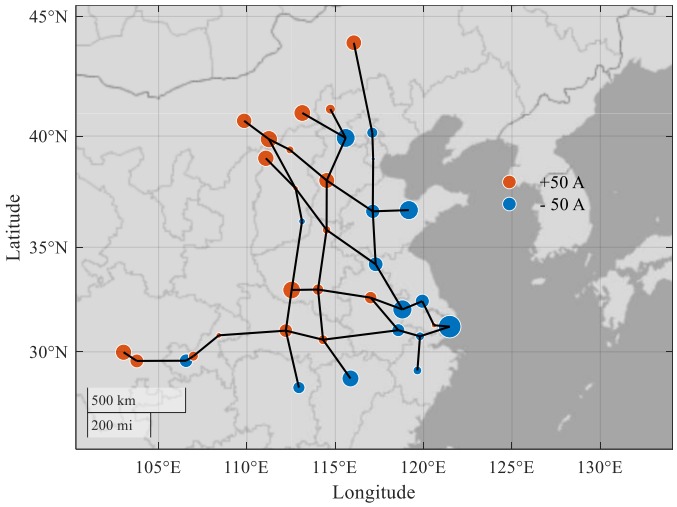

Fig. 5. A snapshot of the GIC distribution in Sanhua grid at the moment of the largest GIC during the GMD event on July 15-16, 2000. (The positive GIC indicates it flow into the earth from the neutral point of the substation.)

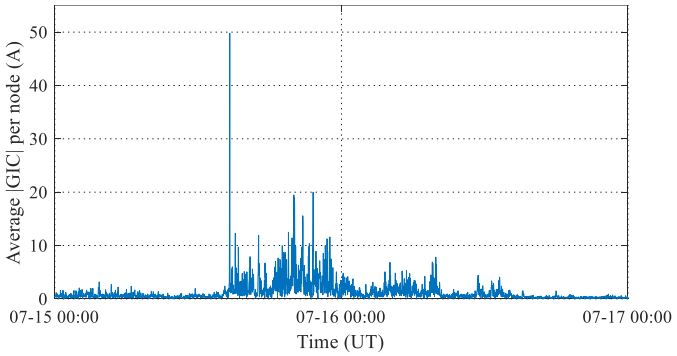

Fig. 6. Time series of average GIC in Sanhua grid during the GMD event on July 15-16, 2000.

V. CONCLUSION

The 10,000-year GMD scenario is established by combining extreme value statistics and theoretical upper limit method, which may provide a useful reference for risk assessment and mitigation measures for critical assets in power system. However, the confidence interval of the 10,000-year return level is relatively wide due to limited amount of geomagnetic data at BMT and characteristics of extreme value analysis. For further study, this will be improved by combining with other data sources, such as geomagnetic indices and geomagnetic data sets at observatories with higher measuring frequency and at similar magnetic latitudes.

ACKNOWLEDGMENT

For the geomagnetic data at BMT observatory used in this paper, we gratefully acknowledge the SuperMAG ground magnetometer data (http://supermag.jhuapl.edu/info/?page=acknowledgement). This work is also supported by the HPC platform at Xi'an Jiaotong University. The authors gratefully acknowledge the support of K.C. Wang Education Foundation, Hong Kong.

REFERENCES

[1] D. H. Boteler and R. J. Pirjola, "Modeling geomagnetically induced currents," *Space Weather*, vol. 15, pp. 258-276, 2017.

[2] "2012 special reliability assessment interim report: Effects of geomagnetic disturbances on the bulk power system," North Amer. Elect. Rel. Corp., Atlanta, GA, USA, Tech. Rep., Feb. 2012.

[3] "Geomagnetic disturbances: Their impact on the power grid," *IEEE Power Energ. Mag.*, vol. 11, no. 4, pp. 71-78, July-Aug. 2013.

[4] A. Pulkkinen, E. Bernabeu, J. Eichner, C. Beggan, and A. W. P. Thomson, "Generation of 100-year geomagnetically induced current scenarios," *Space Weather*, vol. 10, 2012.

[5] A. W. P. Thomson, E. B. Dawson and S. J. Reay, "Quantifying extreme behavior in geomagnetic activity," *Space Weather*, vol. 9, 2011.

[6] E. J. Oughton, M. Hapgood, G. S. Richardson, C. D. Beggan, A. W. P. Thomson, M. Gibbs, C. Burnett, C. T. Gaunt, M. Trichas, R. Dada, and R. B. Horne, "A risk assessment framework for the socioeconomic impacts of electricity transmission infrastructure failure due to space weather: An application to the United Kingdom," *Risk Anal.*, vol. 39, no. 5, pp. 1022-1043, 2019.

[7] "Extreme space weather: Impacts on engineered systems and infrastructure," Royal Academy of Engineering, London, England, pp. 42, 2013.

[8] S. Guo, L. Liu, R. J. Pirjola, K. Wang, and B. Dong, "Impact of the EHV power system on geomagnetically induced currents in the UHV power system," *IEEE Trans. Power Del.*, vol. 30, no. 5, pp. 2163-2170, Oct. 2015.

[9] Q. Liu, Y. Xie, N. Dong, Y. Chen, M. Liu, and Q. Li, "Uncertainty quantification of Geo-magnetically induced currents in UHV power grid," *IEEE Trans. Electromagn. Compat.*, vol. 62, no. 1, pp. 258-265, Feb. 2020.

[10] S. Coles, "An Introduction to Statistical Modelling of Extreme Values," London: Springer, 2001, pp. 74-91.

[11] E. Gilleland and R. W. Katz, "extRemes 2.0: An Extreme Value Analysis Package in R," *J. Stat. Softw.*, vol. 72, no. 8, pp. 1-39, Aug. 2016.

[12] V. M. Vasyliūnas, "The largest imaginable magnetic storm," *J. Atmos. Sol. Terr. Phys.*, vol. 73, no. 11–12, pp. 1444-1446, 2011.

[13] G. S. Kelly, A. Viljanen, C. D. Beggan, and A. W. P. Thomson, "Understanding GIC in the UK and French high-voltage transmission systems during severe magnetic storms," *Space Weather*, vol. 15, pp. 99-114, 2017.

[14] D. H. Boteler and R. J. Pirjola, "Comparison of methods for modelling geomagnetically induced currents," *Ann. Geophys.*, vol. 32, no. 9, pp. 1177-1187, 2014.

[15] K. Zheng, R. J. Pirjola, D. H. Boteler, and L. Liu, "Geoelectric fields due to small-scale and large-scale source currents," *IEEE Trans. Power Del.*, vol. 28, no. 1, pp. 442-449, 2013.

[16] J. W. Gjerloev, "The SuperMAG data processing technique," *J. Geophys. Res.*, vol. 117, 2012.

[17] E. B. Savage, W. A. Radasky and J. L. Gilbert, "Sudden impulse environment for Cigre technical brochure," 2017 XXXIInd General Assembly and Scientific Symposium of the International Union of Radio Science (URSI GASS), Montreal, QC, 2017, pp. 1-4.

[18] "Understanding of geomagnetic storm environment for high voltage power grids," CIGRE Technical Brochure 780, 2019.

[19] J. G. Kappenman, "Storm sudden commencement events and the associated geomagnetically induced current risks to ground-based systems at low-latitude and midlatitude locations," *Space Weather*, vol. 1, no. 3, 1016, 2003.

[20] D. H. Boteler, Q. Bui-Van and J. Lemay, "Directional sensitivity to geomagnetically induced currents of the Hydro-Quebec 735 kV power system," *IEEE Trans. Power Del.*, vol. 9, no. 4, pp. 1963-1971, Oct. 1994.

[21] "TPL-007-2 - Transmission System Planned Performance for Geomagnetic Events," North Amer. Elect. Rel. Corp., Nov. 2017.